First Asia-Pacific Solar Physics Meeting
ASI Conference Series, 2011, Vol. 2, pp 137–142
Edited by Arnab Rai Choudhuri & Dipankar Banerjee

Alpha effect due to magnetic buoyancy instability of a horizontal magnetic layer

Piyali Chatterjee[1]*
NORDITA, Roslasgtullsbacken 23, AlbaNova University Center, SE-10691, Stockholm, Sweden

Abstract. In this paper we study the hydromagnetic instability of a toroidal magnetic layer such as that thought to be located in the solar tachocline. The magnetic layer is located in a convectively stable layer and is subject to what is known as the magnetic buoyancy instability (MBI) and under suitable conditions breaks up into twisted and arching magnetic flux tubes. The MBI gives rise to an anti-quenched α effect which can be measured by using the sophisticated quasi-kinematic test field method. This paper aims at summarizing the main results of a much longer paper by Chatterjee et al. 2011, A&A (in press).

Keywords : Sun: dynamo – Sun: magnetic topology – instabilities

1. The Model

We consider a set-up similar to Brandenburg & Schmitt (1998) with the computational domain being a cuboid with $L_z = L_x = L_y/3$. The domain has constant gravity g_z pointing in the negative z direction and is rotating with a constant angular velocity $\mathbf{\Omega}$ making and angle θ with the vertical (z). The box may be thought of as being placed at a colatitude θ on the surface of a sphere with $\hat{x}$, $\hat{y}$ and $\hat{z}$ directions pointing along the local θ, ϕ and r in spherical geometry. The base state is a polytrope i.e., $p = C\rho^{\Gamma}$, with index $m = 1/(\Gamma - 1) = 3$. The initial magnetic field is a horizontal layer of thickness $2H_B = 0.1L_z$, where B_y has the profile

$$B_{y0} = B_0 H_{\rm B} \frac{\partial}{\partial z} \tanh\left(\frac{z - z_B}{H_{\rm B}}\right), \quad (1)$$

The atmosphere is suitably adjusted for magneto hydrostatic equilibrium. The reader is requested to refer to Chatterjee et al. (2011) for further details. We solve the set

*email: mppiyali@gmail.com

of resistive MHD equations for density, ρ, velocity, $\vec{U}$, entropy, s and magnetic vector potential $\vec{A}$ using the fully compressible PENCIL CODE [1]. The viscosity, magnetic diffusivity and the temperature conductivity are denoted by ν, η and χ respectively. The Prandtl numbers are defined as $\mathrm{Pr} = \nu/\chi$ and $\mathrm{Pr_M} = \nu/\eta$. Additionally we denote the Roberts number by $\mathrm{Rb} = \chi/\eta$.

2. Results

2.1 Nature of the instability

We have performed a number of runs by varying the Prandtl numbers Pr and $\mathrm{Pr_M}$ for a modified plasma beta, $\tilde{\beta}$ defined as the ratio of the total pressure to the magnetic pressure ~ 1.51. This value of $\tilde{\beta}$ is much higher than expected at the bottom of the convection zone. Nevertheless we have used this value so that the instability shows a clear exponential growth for the grid sizes used. In the linear stage the state vector of the system, $\Psi = \left\{\rho, \vec{v}, s, \vec{B}\right\} \propto \tilde{\Psi}(z) \exp(2\pi i \left\{mx/L_x + ny/L_y\right\} - i\omega t)$, where m, n are integers and $\omega = \omega_R + i\omega_I$. Dispersion relations $\omega(m, n)$ have been found for anelastic and non rotating system by Fan (2001) and for rotating systems under magnetostrophic approximation by Schmitt (1985). We obtain 'undular' modes for $5 \le m \le 8$ and $n = 1$. Our findings agree with Thelen (2000) where for moderate rotation the fastest growing mode always has the smallest possible wavenumber in the direction of initial magnetic field and higher wavenumber perpendicular to it. The temporal evolution of the instability can be clearly separated into an initial exponentially growing phase and a subsequent saturation phase with slow decay on resistive timescale as shown in Fig. 1. Even though the initial field is in the y direction, along the course of evolution the orthogonal components B_x and B_z are generated. In absence of shear this implies existence of an α-effect. We also note that the growth rate of the instability increases with increasing Rb of the set up (left panel of Fig. 2). This means that efficient thermal diffusion makes the sub-adiabatically stratified system more unstable to buoyancy instability. This is in agreement to that found by Acheson (1979). In order to provide a better idea of the 3D geometry of the instability in the early saturated phase, we provide in Fig. 3, a volume rendering of constant B_y and field line topology of the magnetic field for two different $\mathrm{Pr_M}$. Note the striking difference in the nature of corrugation of the B_y isosurface. We attribute this to the larger amount of twist for the case with $\mathrm{Pr_M} = 0.5$ compared to the case with $\mathrm{Pr_M} = 0.125$. In terms of the Roberts number, Rb this means that simulations with a larger Rb i.e., more efficient thermal diffusion compared to magnetic diffusion acquire more twist (Fig. 2 right panel). This is an important outcome of our study.

[1] `http:\\pencil-code.googlecode.com`

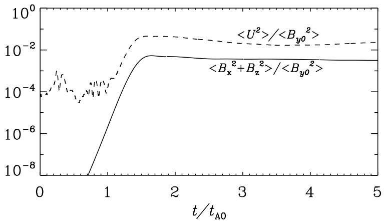

Figure 1. Mean squared values of scaled velocity and generated magnetic field components B_x, B_z for a run with (Pr = $\mathrm{Pr_M}$ = 1) as a function of time also scaled by the initial Alfvén travel time, t_{A0} along y direction. Note the clear exponential growth until $t \approx 1.4t_{A0}$. Fast oscillations in $\langle U^2\rangle$ until $t \approx t_{A0}$ indicate g–modes originating from the initial velocity perturbation.

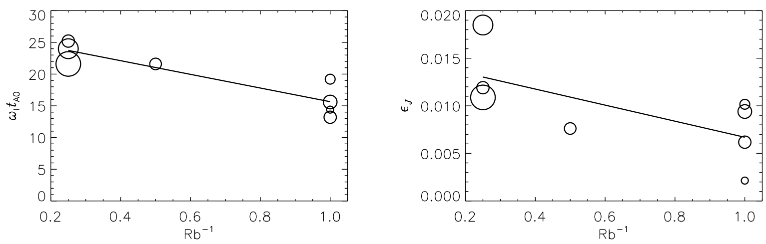

Figure 2. Dependence of growth rate ω_I (left panel) and dependence of the total relative current helicity ϵ_J (right panel) on inverse Roberts number. Solid line: best linear fit.

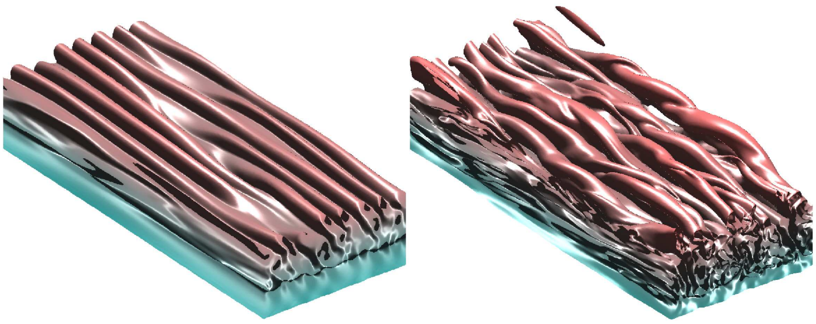

Figure 3. Volume rendering of the $B_y = 0.1B_0$ isosurface for Pr = 0.125, $\mathrm{Pr_M}$ = 0.125 (left). and for Pr = 0.125, $\mathrm{Pr_M}$ = 0.5 (right) at $t = 2t_{A0}$ (saturated stage).

2.2 Calculation of turbulent transport coefficients or α and η tensors

The turbulence resulting from the buoyancy instability generates a mean magnetic field component $\overline{B}_x$ from an initial $\overline{B}_y$ which is also modified compared to its ini-

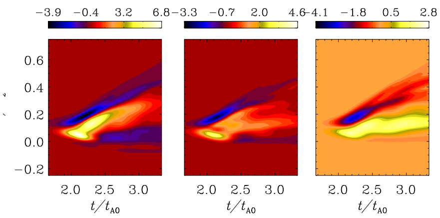

Figure 4. Reconstruction of the mean EMF using $\hat{\alpha}$ and $\hat{\eta}$ from the test-field method. $\overline{\mathcal{E}}_y(z,t)$, scaled by $10^{-4}B_0^2$. Left: directly from $\overline{\mathbf{u}\times\mathbf{b}}$. Middle: Reconstruction using Fourier amplitude of the modes $k' = 0.5, 1, 1.5, ...16$ of the mean field, $\overline{B}_y$. Right: Same as before, but using only the $k' = 0.5$ contribution

tial shape. The mean fields denoted by an overbar are defined as horizontal averages and are only functions of z. We employ the quasi-kinematic test-field (QKTF) method (Schrinner et al. 2005, 2007) to calculate transport coefficients like the $\boldsymbol{\alpha}$ and $\boldsymbol{\eta}$ tensors which describe this process. So far, the method has mostly been applied in situations where a hydrodynamic background was already present in absence of the mean magnetic field (see, e.g. Brandenburg A., Rädler K.-H. & Schrinner M., 2008). The only peculiarity occurring here is the fact that all components of $\boldsymbol{\alpha}$ and $\boldsymbol{\eta}$ vanish for $0 \le B_{\rm rms} \le B_{\rm threshold}$, because fluctuating velocity and magnetic fields develop only after the instability has set in. Another aspect not considered in most previous test-field studies is the strong intrinsic inhomogeneity of the turbulence not only as a consequence of the strong z dependence of B_y, but also due to the stratified density background. Thus the transport coefficients need to be determined as z dependent quantities. Apart from this the transport coefficients are also non local since they depend upon the wavenumber, k' of the test field employed to probe the resulting hydromagnetic turbulence. The reader is requested to look at Chatterjee et al. (2011) for details of the method. Further we have verified that the QKTF method is applicable to our specific problem by reconstructing the turbulent emf (defined as $\overline{\mathbf{u}\times\mathbf{b}}$) from the turbulent transport coefficients we calculate. Here $\mathbf{u}$ and $\mathbf{b}$ denote the fluctuating components of the velocity and the magnetic field. Note that here $\boldsymbol{\alpha}(z,k')$ and $\boldsymbol{\eta}(z,k')$ are 2×2 tensors. Our reconstruction of the y component of the mean emf, $\overline{\mathcal{E}}_y$ is demonstrated in Fig. 4.

2.3 Dependence on rotational inclination

We expect the growth rate of the instability to decrease from the equator to the pole (Schmitt 2003). This can be explained by the buoyant nature of the turbulence, for which vertical motions are essential: At the poles, the effect of the Coriolis force on them is weakest whereas they are strongly deflected at the equator. This is indeed confirmed by the left panel of Fig. 5, where the growth rate is seen to increase continuously when changing λ from 0° (pole) towards 90° (equator). In the context of

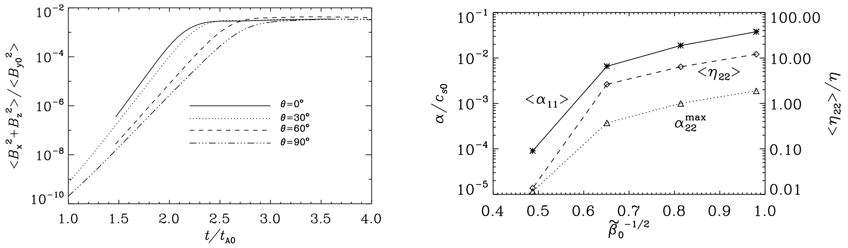

Figure 5. Left: Dependence of the instability on rotational inclination θ in terms of rms value of generated field components $\langle B_x^2 + B_z^2 \rangle$. Right: Vertical averages of $\hat{\alpha}_{11}/c_{s0}$ (solid) and $\hat{\eta}_{22}/\eta$ (dashed) for $k' = 0.5$ at $t = t^{sat}$ and maximum of $\hat{\alpha}_{22}$ with respect to all z and t (dotted) as functions of $\tilde{\beta}^{-1/2} \propto B_0$.

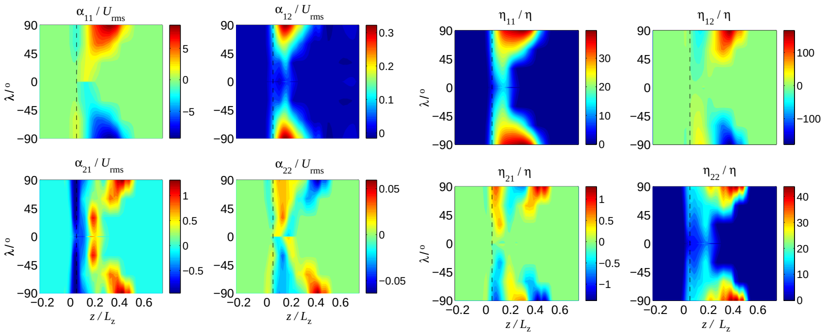

Figure 6. $\hat{\boldsymbol{\alpha}}(z, \lambda)$ and $\hat{\boldsymbol{\eta}}(z, \lambda)$ with $\Omega \neq 0$, calculated using test fields with $k' = 0.5$ just after saturation. $\hat{\boldsymbol{\alpha}}$ scaled by U_{rms}, $\hat{\boldsymbol{\eta}}$ scaled by the molecular diffusivity η. Dashed line: initial position of the magnetic layer.

the solar dynamo problem it is imperative to look at the distribution of $\boldsymbol{\alpha}$ and $\boldsymbol{\eta}$ with rotational inclination θ or latitude, $\lambda = 90° - \theta$ (Fig. 6).

2.4 Dependence on initial magnetic field strength or anti-quenching

In standard mean-field theory for a prescribed hydrodynamic background the turbulent transport coefficients usually decrease as the mean magnetic field increases ("quenching"). The present problem is different, however, because the instability and hence the turbulence is just caused by the initial (mean) magnetic field. In the right panel of Fig. 5, we show the dependence of some of the transport coefficients as a function of the initial field B_0 plotted. Clearly, $\hat{\alpha}_{11}$, $\hat{\alpha}_{22}$, and $\hat{\eta}_{22}$ increase with the initial magnetic field strength supporting earlier ideas of a possible "anti-quenching" in the case of the buoyancy instability (see, e.g., Brandenburg et al. 1998). Note, however, that the dependence on the initial field strength in the right panel of Fig.5 might differ from the dependence on the local field strength to which the term “quenching” usually refers.

3. Conclusions

Our simulations of magnetic buoyancy instability of a strong toroidal field layer in a stratified atmosphere reveals that: (1) The growth rate of the instability and the twist of the resultant flux tubes depend on the Roberts number, Rb of the set up. The 3D nature of the resulting turbulence gives rise to an α effect which generates $\overline{B}_x$ from an initial $\overline{B}_y$ field. (2) The turbulent mean emf can be reproduced reasonably well using the transport coefficients α and η calculated using the quasi kinematic test field method. The components of α and η are non local and inhomogeneous. (3) The growth rate of MBI depends strongly on rotational inclination θ and so does the transport coefficients. (4) This system is an example of anti-quenching where the transport coefficients increase with increasing initial field strength in contrast to hydrodynamic turbulence which is suppressed by strong magnetic fields.

Acknowledgements

The computations have been carried out on the National Supercomputer Centre in Linköping and the Center for Parallel Computers at the Royal Institute of Technology in Sweden. This work was supported by the European Research Council under the AstroDyn Research Project No. 227952.

References

Acheson D. J., 1979, Solar Phys., 62, 23
Brandenburg A., Saar S. H., Turpin C. R., 1998, ApJ, 498, L51
Brandenburg A., Schmitt D., 1998, A&A, 338, L55
Brandenburg A., Rädler K.-H., Schrinner M., 2008, A&A, 482, 739
Chatterjee P., Mitra D., Rheinhardt M., Brandenburg A., 2011 A&A in press, eprint arXiv:1011.1218
Fan Y. 2001, ApJ, 546, 509
Schmitt D., 1985, Dynamowirkung magnetostrophischer Wellen (PhD thesis, University of Göttingen)
Schrinner M., Rädler K.-H., Schmitt D., Rheinhardt M., Christensen U., 2005, Astr. Nachr., 326, 245
Schrinner M., Rädler K.-H., Schmitt D., Rheinhardt M., Christensen U., 2007, GAFD, 101, 81
Thelen J. C., 2000, MNRAS, 315, 155